agriculture

MDPI

Article

Experimental Study on the Mechanical Properties of Friction, Collision and Compression of Tiger Nut Tubers

Shengwei Zhang [1], Jun Fu [1,2], Ruiyu Zhang [1], Yan Zhang [1] and Hongfang Yuan [1,2,*]

[1] College of Biological and Agricultural Engineering, Jilin University, Changchun 130022, China; zsw21@mails.jlu.edu.cn (S.Z.); fu_jun@jlu.edu.cn (J.F.); zhangry20@mails.jlu.edu.cn (R.Z.); zhang_yan21@mails.jlu.edu.cn (Y.Z.)
[2] Key Laboratory of Bionic Engineering, Ministry of Education, Jilin University, Changchun 130022, China
* Correspondence: yuanhongfang@jlu.edu.cn; Tel.: +86-151-0442-8212

Abstract: The mechanical properties of agricultural materials can provide the basis for the design and optimisation of agricultural machinery. There are currently very few studies on the mechanical properties of tiger nut tubers, which is not conducive to the design and development of machinery for their harvesting and processing. To obtain the mechanical parameters of tiger nut tubers, this study investigated the effects of variety (Zhong Yousha 1 and Zhong Yousha 2), moisture content (8%, 16%, 24%, 32% and 40%), contact material (steel, aluminium, plexiglass and polyurethane), release height (170 mm, 220 mm, 270 mm and 320 mm), loading speed (5 mm/min, 10 mm/min, 15 mm/min and 20 mm/min), compression direction (vertical and horizontal) on the friction, collision and compression mechanical properties of the tubers. The results were as follows: Both moisture content and contact material had a significant effect ($p < 0.01$) on the sliding friction coefficient (0.405–0.652) of the tubers; both variety and moisture content had a significant effect ($p < 0.01$) on the angle of repose (27.96–36.09°); contact material, moisture content, release height and variety all had a significant effect ($p < 0.01$) on the collision recovery coefficient (0.376–0.672) of tubers; variety, loading speed, moisture content and compression direction all had significant effects ($p < 0.01$) on the damage force (87.54–214.48 N), deformation (1.25–6.12 mm) and damage energy (82.38–351.08 mJ) of the tubers; only moisture content and compression direction had significant effects ($p < 0.01$) on the apparent elastic modulus (12.17–120.88 MPa) of the tubers. The results of this study can provide a reference for the design and optimisation of machinery for the harvesting and processing of tiger nut tubers.

Keywords: tiger nut; sliding friction coefficient; angle of repose; collision recovery coefficient; compression mechanical properties

Citation: Zhang, S.; Fu, J.; Zhang, R.; Zhang, Y.; Yuan, H. Experimental Study on the Mechanical Properties of Friction, Collision and Compression of Tiger Nut Tubers. *Agriculture* **2022**, *12*, 65. https://doi.org/10.3390/agriculture12010065

Academic Editor: Francesco Marinello

Received: 1 December 2021
Accepted: 4 January 2022
Published: 5 January 2022

1. Introduction

Tiger nut (*Cyperus esculentus* L.) is a high-quality, high-yield, comprehensive use of high-value sedge plant; its growth is extremely adaptable, it can be planted in the sand and land, and it also plays a role in land improvement, wind and sand control, and protection of the ecological environment [1–3]. The oil content of tiger nut tubers is about 25%, and the oil yield per unit area is four times that of soybeans and two times that of rape; the oil meal, a by-product of oil extraction, is a high-quality feed alternative to maize; the above-ground stems and leaves can be used as green fodder, green manure, paper-making, or packaging materials; and the tubers can also be processed to make edible snacks, etc. [4]. Since the comprehensive use of tiger nuts is of high value, the development of the tiger nut industry is of great significance in improving the self-sufficiency rate of edible oil in China and ensuring national food and oil security.

Tiger nut tubers grow underground and have a well-developed root system. During harvesting, the roots, stems, leaves, fruits, and soil are excavated in one piece, followed

by fruit picking and cleaning; the harvested tubers are then polished, dried, and peeled. During the harvesting and processing process, the tubers and the working parts inevitably generate friction, collision, and extrusion resulting in mechanical damage, and the damaged tubers are prone to mould and rot, thus, shortening the storage period and reducing the edible quality, which seriously restricts the development of the tiger nut industry [5]. During harvesting and processing of tiger nut tubers, factors such as moisture content and mechanical material have an influence on their friction coefficient, collision recovery coefficient, and compression mechanical properties [6,7], Therefore, the determination of the friction, collision, and compression mechanical characteristics of tiger nut tubers under different factors such as moisture content can provide a parameter basis for the design and optimisation of tiger nut harvesting and processing machinery, effectively reducing the damage rate during mechanised harvesting and processing, and improving economic efficiency.

In order to provide a parametric basis for the design of agricultural implements, scholars at home and abroad have conducted studies on the mechanical properties of friction, collision, and extrusion of a wide range of agricultural crops. Chen et al. [8] used the discrete element method to model maize and wheat, and calibrated the sliding friction and recovery coefficients for both particles. Chandio et al. [9] studied the effects of moisture content and loading speed on the compressive mechanical properties of maize and showed that the kernel rupture force was negatively correlated with moisture content and loading speed, respectively. Feng et al. [10–12] studied the effects of release height, collision material, moisture content, fall direction, variety, and mass on the collision recovery coefficient of potato tubers, and the results showed that, except for fall direction and variety, collision material, release height, tuber mass, and moisture content, in that order, had significant effects on the recovery coefficient. Yang et al. [13] conducted a study on the compressive mechanical and frictional properties of grains with different moisture contents and found that as the moisture content increased, the damage force and apparent elastic modulus of grains decreased, the deformation and damage energy showed first a decrease and then an increase, and the friction coefficient increased. Gao et al. [14] studied the mechanical properties of soybeans in static compression, revealing the mechanical damage mechanism of soybeans at different moisture contents and different compression directions. Arslan et al. [15] investigated the compressive mechanical properties of almonds and found that the damage force, deformation, damage energy, and compressive power of almonds in different compression directions decreased with increasing moisture content. In addition, the mechanical properties of walnuts [16], lotus seeds [17], rice [18], and peanuts [19] have all been studied, while little research has been reported on tiger nut tubers.

In conclusion, research on the friction, collision, and compression mechanical properties of tiger nut tubers at home and abroad has lagged behind that of other crops, and research on tiger nut tubers has focused more on their composition analysis and extraction [20–23], edible value [24–26], processing and storage [27–30], and cultivation [31–34]. Therefore, tiger nut tubers were used as an object of study in this research, and friction, collision and compression mechanical tests were carried out on the tubers; then, the effects of factors such as moisture content on its sliding friction coefficient, collision recovery coefficient and damage force, deformation, damage energy, and apparent elastic modulus were analysed to provide theoretical parameters for the design and optimisation of machinery for tiger nut tuber harvesting and processing.

2. Materials and Methods

2.1. Test Materials

The test materials for this study were selected from two high oil and high yielding varieties, Zhong Yousha 1 (V.1) and Zhong Yousha 2 (V.2), both from Dingzhou City, Hebei Province, China. Tiger nut tubers in their harvesting stage were hand-dug and selected free of pests and damage as test samples.

As moisture content is a common factor affecting the friction, collision, and compression mechanics of tiger nut tubers, samples of tubers with different moisture contents needed to be prepared to facilitate subsequent tests. The moisture content of both tubers was measured at approximately 40% at harvest using the constant temperature drying method, while the moisture content of the tubers during processing was about 10%, so the tuber moisture content range was set at 8% to 40%. Tubers with a moisture content of 40% were used as the base sample. For tubers with the desired moisture content below 40%, the base sample was dried in a blast drying oven at a constant temperature of 40 °C, and the moisture content was measured every 30 min using a moisture capacity meter; and the tubers that reached the desired moisture content were placed in a fresh bag and stored in a crisper at a low temperature of 4 °C. Samples with moisture contents of 8%, 16%, 24%, 32%, and 40% were obtained by drying.

In total, 1000 tubers of different moisture contents were randomly selected, and their thousand grain weight was measured using an electronic balance with an accuracy of 0.01 g. The tubers were freely filled in a cylindrical container (inner diameter 66 mm, height 150 mm), and their bulk density (the ratio of the mass of the filled tubers to the volume of the container) was calculated. The triaxial sizes of the tubers (length L, width W, and thickness T) were measured by vernier calipers as shown in Figure 1; the results were taken as the mean value and their sphericity φ was calculated according to Equation (1). The results of their basic physical parameters are all shown in Table 1.

$$\varphi = \frac{\sqrt[3]{(L \cdot W \cdot T)}}{L} \times 100\% \quad (1)$$

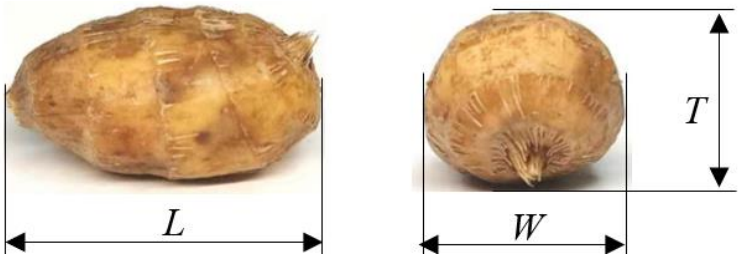

Figure 1. Triaxial size of the tiger nut tuber.

Table 1. Basic physical parameters of tiger nut tubers.

Variety	Moisture Content/%	Triaxial Size/mm			1000 Grain Weight/g	Bulk Density/(g·cm^{-3})	Sphericity/%
		Length	Width	Thickness			
V.1	8	14.51	13.90	10.71	1072.72	9.31	89.09
	16	15.44	14.52	10.89	1230.14	9.21	87.21
	24	15.58	14.78	11.61	1318.58	9.13	89.08
	32	15.61	14.75	11.80	1505.98	9.12	89.39
	40	16.03	15.13	12.24	1658.93	9.08	89.66
V.2	8	21.65	14.12	11.29	1606.40	9.52	69.80
	16	23.01	14.27	11.43	1800.48	9.36	67.54
	24	23.19	14.56	12.18	2097.73	9.38	69.09
	32	23.22	14.57	12.57	2290.58	9.35	69.77
	40	23.95	14.93	12.61	2544.08	9.24	68.98

2.2. Test Device and Method

2.2.1. Friction Properties Test

The sliding friction coefficient and the angle of repose are two important parameters that reflect the frictional characteristics of bulk materials, which are related to factors such as the moisture content of the material and its external dimensions. As shown in

Figure 2, the sliding friction coefficients between tubers with different moisture contents and steel, aluminium, plexiglass, and polyurethane were determined using a homemade inclinometer [35]. Due to the large sphericity of the tuber, in order to prevent the tuber from rolling, the test used glue to bond the four tubers together and placed them on the friction material, slowly lifting the inclinometer at a uniform speed to make it inclined. When the tuber was at rest on the inclined surface, it was subjected to gravity, static friction, and support force; when the inclination angle α of the inclined surface increased to cause the surface object to begin to slide, the sliding friction coefficient μ_s then was:

$$\mu_s = \tan\alpha \tag{2}$$

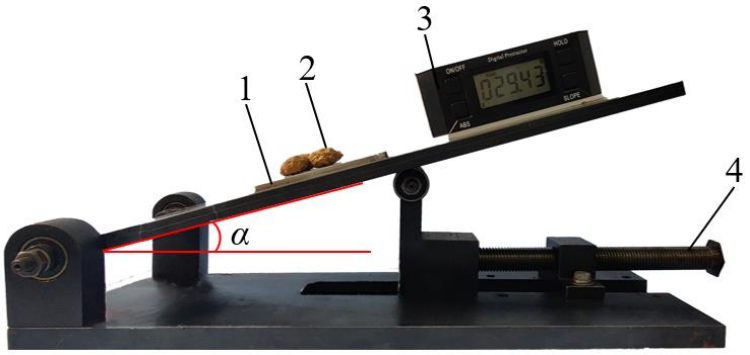

Figure 2. Test device for sliding friction coefficient. 1. Friction material; 2. Tuber plate; 3. Angle tester; and 4. Bevelled push-up screw.

As shown in Figure 3, the angle of repose test was carried out on tiger nut tubers using the cylinder lifting method. To reduce the effect of friction between the cylinder material and the tuber on the angle of repose of the tuber, the cylinder was made of smooth stainless steel with an inner diameter of 60 mm, a height of 150 mm, and a thickness of 1.5 mm. The test was carried out by filling the entire cylinder with tubers and then lifting it slowly and uniformly to allow the tubers to accumulate naturally until they were stable. At the end of the test, images of the piles were taken, the edge curves of the piles of tubers were extracted using Matlab software and a linear fit was made, with the angle β between the fitted line and the horizontal plane being the angle of repose.

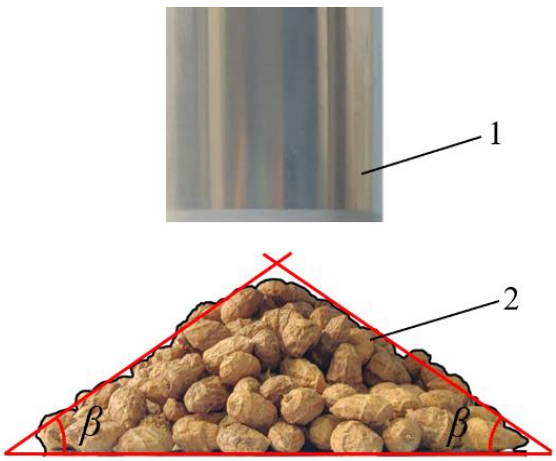

Figure 3. Test device for angle of repose measurement and image processing. 1. Cylinder and 2. Image of tuber accumulation.

Each of the above tests was repeated 10 times, and the results were averaged.

2.2.2. Collision Properties Test

The collision recovery coefficient is one of the most important indicators for evaluating the collision properties of bulk materials and is used to measure the ability of the material to recover from deformation after collision. It is defined as the ratio of the instantaneous separation velocity normal to the point of contact after an object collision to the contact velocity at the time of the collision.

As shown in Figure 4, a combination of free-fall collision and high-speed camera was used to determine the collision recovery coefficient of the tubers [36]. The test system consisted of a vacuum straw, collision material plate, grid paper, high-speed camera (Phantom v711, Vision Research, Wayne, NJ, USA), and fill light. As shown in Figure 5, the vacuum suction tube was adjusted to the desired test height, the suction tube was used to adsorb the tuber to be tested, then the vacuum pump was turned off and the tuber was free to fall and collide with the material plate, the initial maximum bounce height of the tuber after the collision was obtained using a high-speed camera. Each set of tests was repeated 20 times (if a large lateral deflection occurred when the tuber rebounded, the test was considered invalid, and the measurement had to be repeated), and the results were calculated using Equation (3).

$$e = \frac{v_1}{v_0} = \frac{\sqrt{2gh}}{\sqrt{2gH}} = \sqrt{\frac{h}{H}} \tag{3}$$

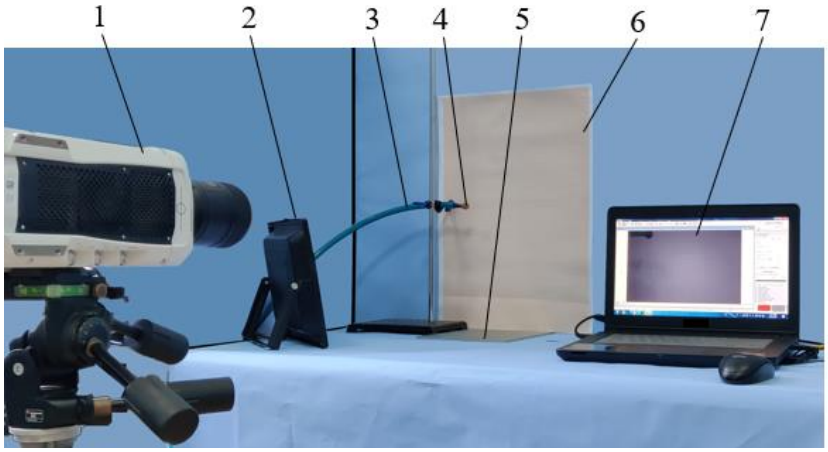

Figure 4. Test device for collision recovery coefficient. 1. High-speed camera; 2. Fill light; 3. Vacuum suction tube; 4. Tuber; 5. Collision material; 6. Grid paper; and 7.PCC.

Initial release First collision Highest point of collision

Figure 5. Test process for collision recovery coefficient.

Note: e is the collision recovery coefficient between the tuber and the material; v_1 is the instantaneous separation velocity of the tuber after collision in the normal direction; v_0

is the instantaneous contact velocity of the tuber collision; h is the maximum height of the tuber rebounding from collision with the material; and H is the release height.

From the literature [15], it is clear that the collision recovery coefficient is related to numerous factors. In this study, moisture content, collision material, release height, and tuber variety were used as test factors, and the tuber collision recovery coefficient was used as a test index, and the $L_{16}(4^3 \times 2^2)$ orthogonal table was selected for a mixed orthogonal test study to determine the significance of the effect of each factor on the recovery coefficient. This was followed by a single-factor test of each significant factor to analyse the rule of influence of each factor on the tuber recovery coefficient. Table 2 shows a table of factor levels for the mixed orthogonal test of the collision recovery coefficient.

Table 2. Table of factor levels for mixed orthogonal tests of collision recovery coefficients.

Level	Moisture Content/%	Collision Material	Release Height/mm	Variety
1	16	Steel	170	V.1
2	24	Aluminium	220	V.2
3	32	Plexiglass	270	/
4	40	Polyurethane	320	/

The results of the mixed orthogonal test showed that all four factors had a significant effect on the recovery coefficient, so a single-factor test was conducted on the four factors, with moisture content test levels of 8%, 16%, 24%, 32%, and 40%; release heights of 150 mm, 200 mm, 250 mm, 300 mm, and 350 mm; and collision materials of steel, aluminium, plexiglass, and polyurethane (all 4 mm thick).

2.2.3. Compression Mechanical Properties Test

As shown in Figure 6, the WDW-20 electronic universal testing machine produced by the Jinan Era Testing Instrument Company (Jinan, China) was used for the compression mechanical properties test, mainly consisting of a supporting pressure head, sensor, control system, etc. The range of the sensor is 0 to 1000 N, the accuracy of the force display is 0.01 N, and the speed range is 0.005 to 500 mm/min. The test force, deformation, and other parameters can be displayed in real time during the test operation.

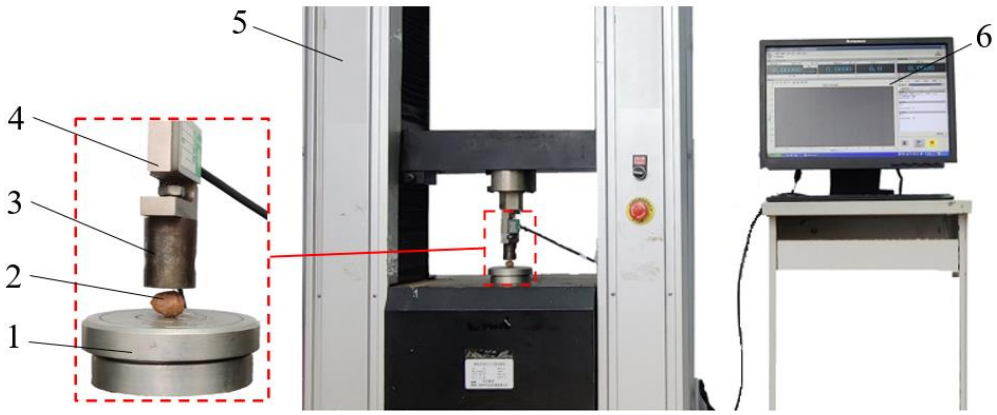

Figure 6. Test system for compression mechanical properties. 1. Carrier table; 2. Tiger nut tuber; 3. Indenter; 4. Sensor; 5. Test mainframe; and 6. Control and display system.

During the test, the specimen to be tested was placed on the carrier table, and then the upper indenter was adjusted downwards so that when the upper indenter touched the sample, it moved downwards at the speed required for the test. The display system recorded the pressure–deformation curve in real time. When there was a significant abrupt change in the pressure value (vertical coordinate) on the curve, it showed that the sample had been cracked and the loading was stopped. The damage force, deformation, damage

energy, and apparent elastic modulus of the tuber under test were obtained by subsequent processing [9]. Each set of tests was repeated 25 times, and the results were averaged.

The apparent elastic modulus can be calculated according to the following formula:

$$E = \frac{0.338F(1-\mu^2)}{d^{3/2}}\left[2K_U\left(\frac{1}{R_U}+\frac{1}{R'_U}\right)^{1/3}\right]^{3/2} \quad (4)$$

$$\cos\theta = (R'_U - R_U)/(R'_U + R_U) \quad (5)$$

Note: E is the apparent elastic modulus of the tuber (MPa); R_U and R'_U are the minimum and maximum radii of curvature of the tuber at the contact point of the upper platen, respectively (mm); F is the compression force (N); d is the deformation of the tuber (mm); μ is the Poisson's ratio of the tuber, and with reference to the Poisson's ratios of wheat, maize, soybean, peanut, and lotus kernel, the Poisson's ratio of the tuber was chosen to be 0.4; cos θ is the cosine of the angle between the main planes; and K_U is a constant (calculated by calculating cos θ, taken from the ASAE S368.4DEC2000 (R2008) standard).

From the literature [19–21], it is known that the mechanical properties of extrusion are related to factors such as moisture content, compression direction, loading speed, and material variety. Therefore, moisture content, loading speed, compression direction, and tuber variety were selected as the test factors, and the tuber damage force, deformation, damage energy, and apparent elastic modulus were used as indicators for the tests, and the results were analysed for significance. Table 3 shows a table of factor levels for full-scale tests of compression mechanics.

Table 3. Table of factor levels for compression mechanics tests.

Level	Moisture Content/%	Loading Speed/(mm·min^{-1})	Compression Direction	Variety
1	16	5	Vertical	V.1
2	24	10	Horizontal	V.2
3	32	15	/	/
5	40	20	/	/

Note: Vertical direction is the direction of the length of the tuber; horizontal direction is the direction of thickness of the tuber.

3. Results and Discussion

3.1. Results and Analysis of Frictional Properties Tests

The results and significance analysis of the sliding friction coefficient and angle of repose measurements for the tiger nut tubers are shown in Tables 4 and 5, respectively.

Table 4. Results of sliding coefficient friction and angle of repose measurements.

V	MC/%	Sliding Coefficient Friction				AOR/°
		Steel	Aluminium	Plexiglass	Polyurethane	
V.1	8	0.434	0.458	0.494	0.499	27.96
	16	0.459	0.480	0.529	0.560	28.89
	24	0.498	0.514	0.571	0.591	30.11
	32	0.540	0.555	0.621	0.632	33.43
	40	0.573	0.613	0.640	0.646	35.82
V.2	8	0.405	0.449	0.507	0.527	30.31
	16	0.465	0.484	0.532	0.564	31.58
	24	0.506	0.526	0.565	0.605	33.17
	32	0.528	0.537	0.606	0.613	34.45
	40	0.581	0.601	0.632	0.652	36.09

Note: V shows variety; MC shows moisture content and AOR shows the angle of repose.

Table 5. Sliding friction coefficient and angle of repose significance analysis.

Source of Variance	Sliding Coefficient Friction		Angle of Repose	
	***F* Value**	***p* Value**	***F* Value**	***p* Value**
Variety	0.945	0.3385	54.272	<0.0001 **
Moisture content	11.357	<0.0001 **	94.587	<0.0001 **
Friction material	7.150	<0.0009 **	/	/

Note: ** shows the significance at $p < 0.01$.

From Table 5, it can be observed that variety had no significant effect on the sliding friction coefficient, while moisture content and friction material had a highly significant effect on the sliding friction coefficient ($p < 0.01$), and with reference to the *F*-value, it can be seen that the main and secondary factors affecting the sliding friction coefficient were moisture content and friction material in order; variety and moisture content had a significant effect on the angle of repose of the tubers ($p < 0.01$), and the main and secondary factors affecting the angle of repose were moisture content and variety in order.

From Table 4, it can be observed that the sliding friction coefficient increased with increasing moisture content for the same variety of tubers rubbing against the same material, mainly due to the increase in moisture content and the subsequent increase in adhesion between the surface of the tuber and the surface of the friction material. At the same moisture content, the coefficient of friction between the tuber and the polyurethane, plexiglass, aluminium, and steel decreased in this order; the fact that the roughness of these four materials decreases in this order, with roughness *R*a values of 3.3 μm, 2.6 μm, 1.4 μm, and 0.8 μm.

The relationship between the moisture content of the tubers and the coefficient of friction was obtained by fitting using Origin software as shown in Table 6. The sliding friction coefficient is approximately linearly increased with moisture content in the range of 8% to 40%, and the R^2 were all greater than 0.95, indicating a good fitting relationship.

Table 6. Fitting equation between sliding friction coefficient and moisture content.

Variety	Material	Fitting Function	R^2
V.1	Steel	$\mu_s = 0.0045x + 0.3931$	0.994
	Aluminium	$\mu_s = 0.0048x + 0.4085$	0.970
	Plexiglass	$\mu_s = 0.0048x + 0.4558$	0.986
	Polyurethane	$\mu_s = 0.0046x + 0.4758$	0.958
V.2	Steel	$\mu_s = 0.0052x + 0.3725$	0.979
	Aluminium	$\mu_s = 0.0045x + 0.4123$	0.964
	Plexiglass	$\mu_s = 0.004x + 0.4712$	0.994
	Polyurethane	$\mu_s = 0.0037x + 0.5025$	0.970

The angle of repose of the tubers of the same variety also increased with increasing moisture content, mainly due to the increase in moisture content, which increases the adhesion between the tubers and tubers and makes them less mobile. When the moisture content was the same, the angle of repose of variety 2 was larger than that of variety 1, because the size of the angle of repose is related to the shape and size of the material, the higher the sphericity of the material, the better its mobility, the smaller the angle of repose. From Table 1, when the moisture content was the same, the sphericity of V.2 was lower than that of V.1 and, therefore, its angle of repose was larger. The relationship between the angle of repose and moisture content of tubers was obtained by fitting the following equation using Origin software.

$$\beta_1 = 0.0056x^2 - 0.0157x + 27.674,\ R^2 = 0.989 \quad (6)$$

$$\beta_2 = 0.1804x + 28.791,\ R^2 = 0.998 \quad (7)$$

Note: β_1 and β_2 represent the angle of repose of V.1 and V.2, respectively, and x represents the moisture content.

Equations (6) and (7) show that the angle of repose of variety 1 had a quadratic polynomial relationship with the moisture content in the range of 8% to 40%, and the angle of repose of variety 2 had a linear increasing relationship with the moisture content, and the R^2 of both equations was greater than 0.98, indicating a good fitting relationship.

From the point of view of friction properties, due to the high moisture content of the tiger nut tubers during the harvesting period, it is advisable to use materials such as polyurethane with a high coefficient of friction for working parts such as the conveyor of the harvester in order to prevent fruit drop. To prevent the accumulation of tubers in the collector box of the harvester, anti-stacking devices such as winches should be added.

3.2. Results and Analysis of Collision Properties Tests

3.2.1. Results and Analysis of Mixed Orthogonal Tests

The scheme and results of the mixed orthogonal test for the collision recovery coefficient of tiger nut tubers are shown in Table 7. Analysis of variance (ANOVA) is shown in Table 8.

Table 7. Scheme and results of the mixed orthogonal test.

Test Number	MC	Collision Material	Release Height	V	Null Column	COR/°
1	1	1	1	1	1	0.503
2	1	2	2	1	1	0.498
3	1	3	3	2	2	0.416
4	1	4	4	2	2	0.404
5	2	1	2	2	2	0.525
6	2	2	1	2	2	0.487
7	2	3	4	1	1	0.408
8	2	4	3	1	1	0.376
9	3	1	3	1	2	0.619
10	3	2	4	1	2	0.595
11	3	3	1	2	1	0.439
12	3	4	2	2	1	0.416
13	4	1	4	2	1	0.672
14	4	2	3	2	1	0.637
15	4	3	2	1	2	0.456
16	4	4	1	1	2	0.396

Note: COR shows the collision recovery coefficient.

Table 8. ANOVA results for the mixed orthogonal test.

Source of Variance	DOF	Mean Square	*F* Value	*p* Value
Variety	3	0.0082	103.414	<0.0001 **
Collision material	3	0.0324	407.857	<0.0001 **
Release height	3	0.0037	46.561	0.0004 **
Variety	1	0.0013	16.558	0.0096 **

Note: ** shows the significance at $p < 0.01$.

As can be seen from Table 8, all four factors had a significant effect ($p < 0.01$) on the collision recovery coefficient of tubers in the following order of significance: collision material, moisture content, release height, and variety.

3.2.2. Results and Analysis of the Single-Factor Test

The results of the single factor test for the collision recovery coefficient are shown in Figure 7.

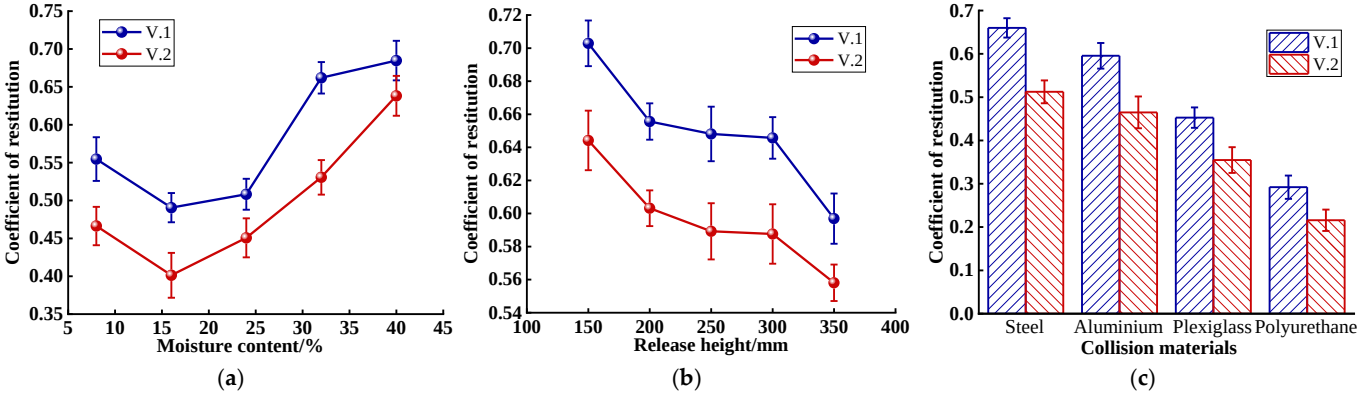

Figure 7. Results of the single factor test for recovery coefficient. (**a**) Effect of moisture content on recovery coefficient; (**b**) Effect of release height on recovery coefficient; and (**c**) Effect of collision material on recovery coefficient. Note: The release height in test (**a**) is 300 mm and the collision material is steel; the moisture content in test (**b**) is 32% and the collision material is steel; the moisture content in test (**c**) is 32% and the release height is 300 mm.

As shown in Figure 7a, the recovery coefficient decreased and then increased with increasing moisture content when tubers of the same varieties were released at the same height and collided with the same material. When the moisture content increased from 8% to 16%, the recovery coefficient decreased from 0.554 to 0.49 for variety 1 and from 0.466 to 0.401 for variety 2. When the moisture content increased from 16% to 40%, the collision recovery coefficient started to increase, from 0.49 to 0.685 for variety 1 and from 0.401 to 0.628 for variety 2. The reasons for this trend are as follows: When the moisture content drops from 40% to 16%, the tuber gradually dries out from full, its hardness and stiffness decrease, its elasticity decreases and its plasticity increases, so the contact deformation increases when it collides with the material, the energy loss becomes larger and the normal velocity after the collision decreases, leading to a decrease in the recovery coefficient; When the moisture content is reduced from 16% to 8%, the tubers crumple, their internal organisation is tighter, their stiffness is enhanced, they are less prone to deformation when colliding with the material, less energy is lost, and therefore their recovery coefficient thus becomes greater. The equation for the recovery coefficient of tubers related to moisture content was obtained by fitting the Origin software as follows.

$$e_1 = -3.4 \times 10^{-5}x^3 + 0.0028x^2 - 0.0636x + 0.9036,\ R^2 = 0.953 \quad (8)$$

$$e_2 = -1.34 \times 10^{-5}x^3 + 0.0014x^2 - 0.0344x + 0.6588,\ R^2 = 0.997 \quad (9)$$

Note: e_1 and e_2 represent the recovery coefficients for variety 1 and variety 2, respectively, and x represents the moisture content.

From the above equation, it can be seen that the relationship between the recovery coefficient and moisture content were both cubic functions, and the R^2 of both equations was greater than 0.95, indicating a good fitting relationship.

The effect of release height on the recovery coefficient was lower than that of collision material and moisture content. As shown in Figure 7b, the recovery coefficient for tubers of the same moisture content, which collided with the same material, all decreased with increasing release height. When the release height is increased from 150 mm to 350 mm, the recovery coefficient decreased from 0.703 to 0.597 for variety 1 and from 0.644 to 0.558 for variety 2. The reason for this is that as the release height increases, the velocity at the moment of collision between the tuber and the material increases, causing greater deformation and energy loss, which reduces the rebound velocity of the tuber and leads to a

reduction in the recovery coefficient. The relationship between the tuber recovery coefficient and release height was obtained by fitting the following equation with Origin software.

$$e_1 = -5.72 \times 10^{-8} H^3 + 4.2922 H^2 - 0.0107 H + 1.5343,\ R^2 = 0.999 \quad (10)$$

$$e_2 = -3.52 \times 10^{-8} H^3 + 2.7383 H^2 - 0.0072 H + 1.2229,\ R^2 = 0.998 \quad (11)$$

Note: H represents the release height of the tuber.

From the above equation, it can be seen that the relationship between the recovery coefficient and release height were both cubic functions, and the R^2 of both equations was greater than 0.99, indicating a good fit.

The collision material had the greatest influence on the recovery coefficient. From Figure 7c, it can be seen that the recovery coefficients resulting from the collision of tubers with different materials had large differences, with the recovery coefficients decreasing between the tubers and steel, aluminium, plexiglas, and polyurethane in that order. The reason for which is that the hardness of the steel is the greatest and the collision energy absorbed by the steel is the lowest when the tuber collides with the steel, while the energy stored in the tuber is the greatest and the stored collision energy is all applied to the rebound after the collision, so the normal velocity generated during the rebound is the greatest, resulting in the greatest recovery factor; whereas aluminium, plexiglass and polyurethane are in decreasing order of hardness, the energy absorption of the materials during the collision is therefore in increasing order, so that the recovery coefficient between the tuber and the polyurethane was the smallest.

Combining Figure 7a–c, it can be seen that the collision recovery coefficient of variety 1 was consistently greater than that of variety 2 in the single-factor test, which is caused by differences in mass and shape. From Table 1, it can be observed that the individual mass of variety 1 was lower than that of variety 2. In the single factor test, ignoring the effect of air resistance, the instantaneous velocities of the two tubers of different masses on collision with the material plate were the same, but the larger the mass of the tuber on collision the greater the deformation and the greater the energy lost. Furthermore, the long spherical tuber (V. 2) had a non-uniform mass distribution compared to the spherical tuber (V. 1) and was prone to rotational deflection during rebound, resulting in a small recovery factor.

From a collision perspective, the influence of tuber moisture content, collision material, release height, and variety differences should be taken into account in the design and manufacture of tiger nut tuber harvesting and processing machinery. For example, in the harvesting process, flexible materials such as polyurethane can be used in the relevant contact parts because of the high moisture content of the tubers, which have a high collision recovery coefficient and are prone to damage upon collision with the working parts. In addition, when sowing, if the distance between the seed outlet and the ground is large, it is easy for the tuber to bounce and shift after colliding with the ground, resulting in a low rate of qualified seed spacing, so the distance between the seed outlet and the ground should be reasonably adjusted.

3.3. Results and Analysis of the Mechanical Properties of Compression

As shown in Figure 8, when the moisture content of variety 2 was 32%, the loading speed was 5 mm/min and the compression direction was horizontal compression, the graph of its compression force versus deformation was obtained through the test. It was found that the trend of the curve of compression force versus deformation obtained from tests conducted according to different combinations of factors was similar to that of Figure 8. During the initial loading stage, the relationship between the compression force and the amount of deformation was approximately linear, and the tuber was predominantly deformed elastically at this stage. When the force reached the first peak point, the force suddenly decreased and then continued to increase; this point was considered the yield point, which means that the microstructure of the tuber was destroyed, and, therefore, the damage force was set to the compression force corresponding to the yield point. The

amount of deformation of the tuber was the horizontal coordinate corresponding to the yield point. The damage energy was the area formed by the curve before the yield point and the horizontal coordinate (red shaded area in Figure 8). After the yield point, the force continued to be loaded, and the curve fluctuated slightly, indicating that local damage to the tuber may occur; the tuber was mainly undergoing plastic deformation at this stage. When the force reached the maximum peak point (rupture point), and then suddenly dropped, this indicated that the tuber was cracked.

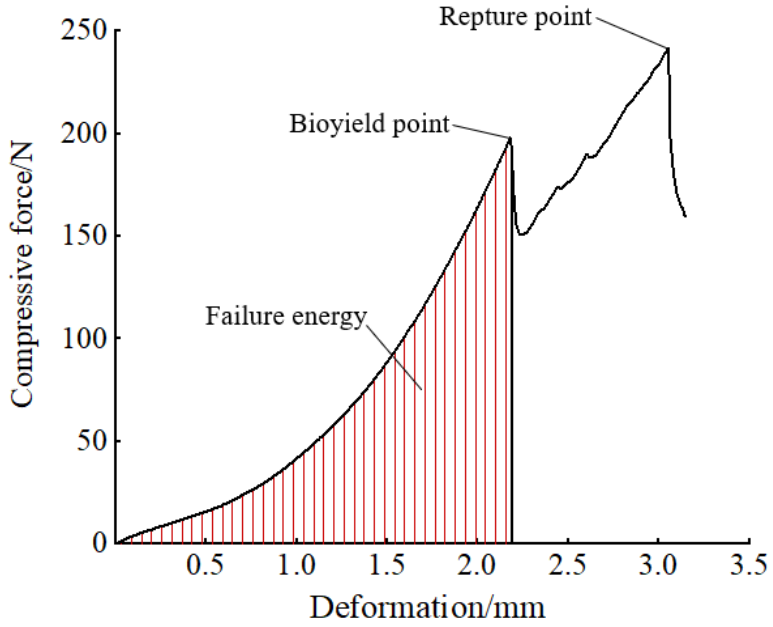

Figure 8. Compressive force–deformation relationship curves for tiger nut tuber.

The test scheme and results of compressive mechanical properties of tubers are given in the Additional materials. For a more visual observation of the test results, Figure 9 has been drawn.

The significance analysis of the results of the compression mechanical properties tests is shown in Table 9.

Table 9. Significance analysis of compressive mechanical properties test results.

Source of Variance	Damage Force		Deformation		Damage Energy		Apparent Elastic Modulus	
	F Value	*p* Value	*F* Value	*p* Value	*F* Value	*p* Value	*F* Value	*p* Value
V	255.164	<0.0001 **	251.172	<0.0001 **	573.150	<0.0001 **	3.515	0.0611
LS	72.560	<0.0001 **	27.271	<0.0001 **	77.151	<0.0001 **	1.034	0.3765
MC	42.238	<0.0001 **	265.070	<0.0001 **	17.969	<0.0001 **	172.592	<0.0001 **
CD	371.794	<0.0001 **	2711.360	<0.0001 **	714.910	<0.0001 **	1275.462	<0.0001 **
V × LS	0.722	0.5387	0.883	0.4491	2.105	0.09785	0.300	0.8258
V × MC	5.451	0.0010 **	16.120	<0.0001 **	9.291	<0.0001 **	18.425	<0.0001 **
V × CD	103.218	<0.0001 **	420.232	<0.0001 **	228.625	<0.0001 **	240.637	<0.0001 **
LS × MC	1.072	0.3806	1.405	0.1809	2.737	0.0036 **	0.991	0.4454
LS × CD	3.293	0.0199 *	0.197	0.8987	1.781	0.1488	1.438	0.2299
MC × CD	13.698	<0.0001 **	43.888	<0.0001 **	8.812	<0.0001 **	10.790	<0.0001 **
V × LS × MC	0.636	0.7669	0.933	0.4954	1.135	0.3346	1.979	0.0384 *
V × LS × CD	3.267	0.0206 *	0.752	0.5210	5.821	0.0006 **	0.451	0.7166
V × MC × CD	1.422	0.2289	9.051	<0.0001 **	2.948	0.0318 *	14.758	<0.0001 **
LS × MC × CD	0.605	0.7938	1.000	0.4377	0.797	0.6193	1.131	0.3371
V × LS × MC × CD	1.267	0.2505	1.398	0.1837	0.439	0.9144	2.657	0.0047 **

Note: ** shows the significance at $p < 0.01$; * shows the significance at $p < 0.05$. V shows variety; LS shows loading speed; MC shows moisture content, and CD shows the the compression direction.

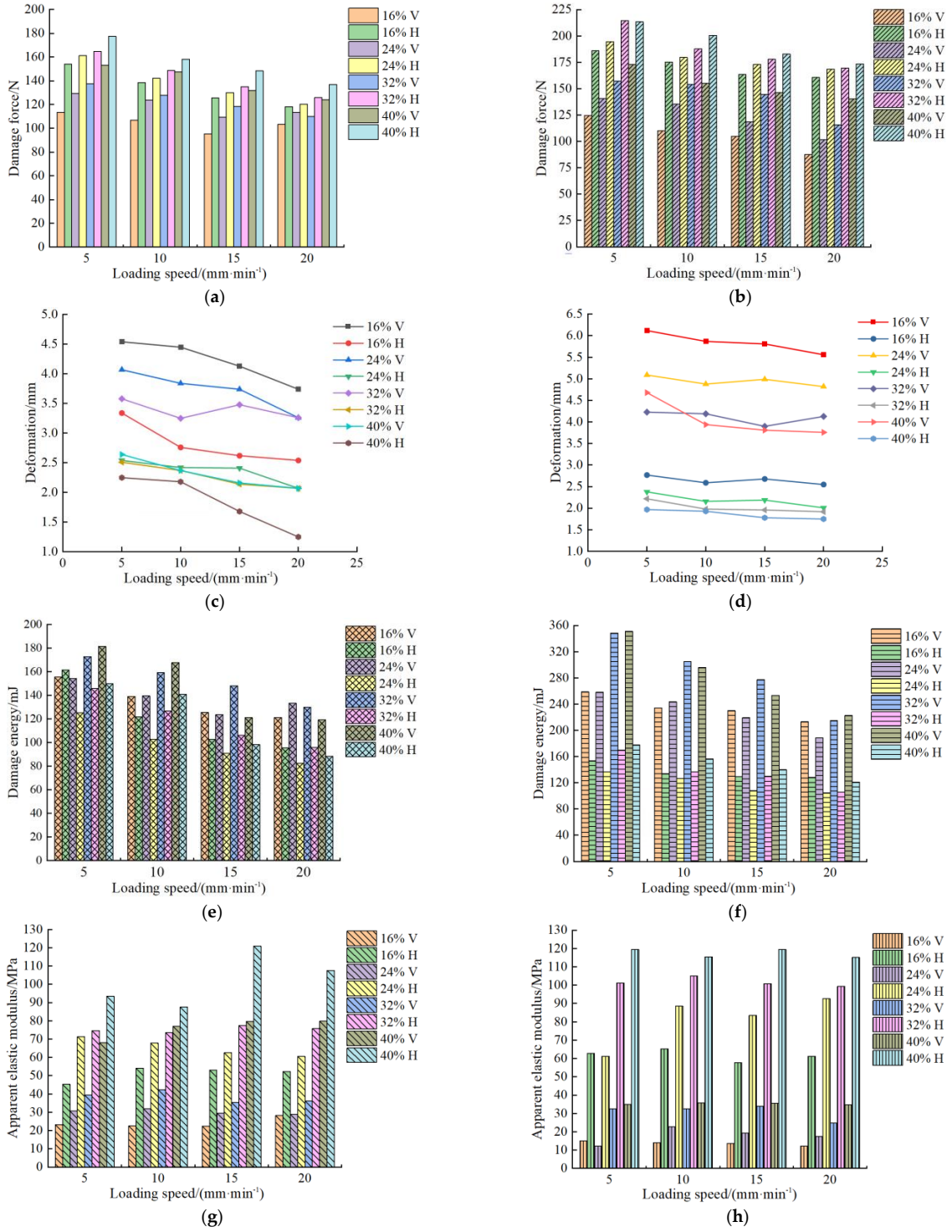

Figure 9. Results of compression mechanical properties tests. (**a**) Effect of factors on the damage force of variety 1 tubers; (**b**) Effect of factors on the damage force of variety 2 tubers; (**c**) Effect of factors on the deformation of variety 1 tubers; (**d**) Effect of factors on the deformation of variety 2 tubers; (**e**) Effect of factors on the damage energy of variety 1 tubers; (**f**) Effect of factors on the damage energy of variety 2 tubers; (**g**) Effect of factors on the apparent elastic modulus of variety 1 tubers; and (**h**) Effect of factors on the apparent elastic modulus of variety 2 tubers. Note: "16% V" and "16% H" mean vertical compression with 16% moisture content and horizontal compression with 16% moisture content respectively, other symbols have similar meanings.

3.3.1. Effect of Loading Speed on Compression Mechanical Properties

From Table 9, it can be observed that the loading speed had a significant effect on the damage force, deformation, and damage energy of the tubers ($p < 0.01$), and no significant effect on the apparent elastic modulus.

As shown in Figure 9, when the level of other factors was fixed (except for the loading rate), as the loading speed increased (from 5 mm/min to 20 mm/min), the damage force, deformation, and damage energy all tended to decrease. As shown in the Table A1 in the Appendix A, when the moisture content was 32% and the loading speed increased from 5 mm/min to 20 mm/min, the damage force of variety 1 in the vertical compression direction decreased from 137.36 N to 109.96 N, the deformation decreased from 3.58 mm to 3.26 mm, and the damage energy decreases from 172.53 mJ to 129.85 mJ; the damage force in the horizontal compression direction decreased from 164.65 N to 125.84 N, the deformation decreases from 2.51 mm to 2.07 mm, and the damage energy decreased from 145.7 mJ to 95.6 mJ.

The reason for the above phenomenon is that when the loading speed is low, the overall force on the tuber is more uniform, the greater the resistance to cracking, the greater the deformation in compression, and the higher the damage energy required. As the loading speed increases, the response time for the internal transfer of forces within the tuber decreases, so that the forces applied to the tuber tend to be concentrated in a certain area, thus making that area the first to produce microstructural damage, and therefore the damage force, deformation, and damage energy are reduced.

3.3.2. Effect of Moisture Content on Compression Mechanical Properties

From Table 9, it can be observed that moisture content had a highly significant effect on the damage force, deformation, damage energy, and apparent elastic modulus of the tubers ($p < 0.01$).

As shown in Figure 9, when the level of factors other than the moisture content is fixed, as the moisture content increased (from 16% to 40%), the damage force and apparent elastic modulus increased, the deformation decreased and the damage energy generally showed a trend of first decreasing and then increasing. As shown in the Table A1 in the Appendix A, when the loading speed was 5 mm/min, and the moisture content increased from 16% to 40%, the damage force of variety 1 in the vertical compression direction increased from 113.44 N to 152.98 N. The deformation decreased from 4.54 mm to 2.64 mm, the damage energy first decreased from 155.18 mJ to 153.98 mJ, then increased to 181.32 mJ, and the apparent elastic modulus increased from 23.21 MPa to 68.12 MPa. The damage force in the horizontal compression direction increased from 153.91 N to 177.47 N, the deformation decreased from 3.34 mm to 2.25 mm. The damage energy first decreased from 161.3 mJ to 125.17 mJ and then increased to 149.65 mJ, and the apparent elastic modulus increased from 45.25 MPa to 93.47 MPa.

The reason for this phenomenon is that when the moisture content was 16%, the tubers were dry, the internal tissues were soft and plastic, the hardness and strength were lower, and the resistance to compression was weaker, so their damage force was lower and the deformation was larger; as the moisture content increased to 40%, the tubers gradually filled up, the hardness and strength increased, and the resistance to deformation and breakage then increased, so the damage force increased and the deformation decreased. The apparent elastic modulus is a measure of the ease of elastic deformation of the tuber and requires a combination of factors such as the shape of the tuber, the state of contact, the compression force, and the amount of deformation. As the damage force increased and the deformation decreased with increasing moisture content, the elastic modulus increased as can be seen from Equation (4).

3.3.3. Effect of Compression Direction on Compression Mechanical Properties

From Table 9, it can be observed that the compression direction had a significant effect on the damage force, deformation, damage energy, and apparent elastic modulus of the tubers ($p < 0.01$).

As shown in Figure 9, when the level of factors other than the direction of compression was fixed, the damage force and apparent modulus of elasticity in the vertical direction were lower than in the horizontal direction, while the deformation and damage energy were generally greater than in the horizontal direction. As shown in the Table A1 in the Appendix A, when the loading speed was from 5 mm/min to 20 mm/min and the moisture content was from 16% to 40%, in the vertical compression direction, variety 1 had a damage force of 95.12 N to 152.98 N, a deformation of 2.07 mm to 4.54 mm, a damage energy of 118.92 mJ to 181.32 mJ and an apparent elastic modulus of 22.43 MPa to 79.79 MPa; in the horizontal compression direction, variety 1 had a damage force of 118.21 N to 177.47 N, a deformation of 1.25 mm to 3.34 mm, a damage energy of 82.38 mJ to 161.3 mJ and an apparent elastic modulus of 45.25 MPa to 120.88 MPa. In the vertical compression direction, variety 2 had a damage force of 87.54 N to 172.81 N, a deformation of 3.76 mm to 6.12 mm, a damage energy of 188.53 mJ to 351.08 mJ, and an apparent elastic modulus of 12.17 MPa to 35.79 MPa; in the horizontal compression direction, variety 2 had a damage force of 160. 56 N to 214. 48 N, a deformation of 1.75 mm to 2.77 mm, a damage energy of 104.53 mJ to 177.67 mJ, and an apparent elastic modulus of 57.75 MPa to 119.37 MPa.

The main reasons for this phenomenon are as follows: When compressed horizontally, the tuber was in a horizontal posture, its transverse cross-sectional area was larger, its stresses were more uniform, its load-bearing capacity was higher, and it was, therefore, more resistant to damage and deformation. However, when compressed vertically, the tuber was in a vertical posture, its transverse cross-sectional area was smaller, it was prone to stress concentration and, therefore, the tuber was prone to rupture and less able to resist deformation. The damage force in the vertical compression was less than in the horizontal compression, but the damage energy was generally greater than in the horizontal compression, mainly because the deformation in the vertical compression was greater than in the horizontal compression, and the energy required was higher. The apparent elastic modulus of the tuber was lower in the vertical compression than in the horizontal compression, which means that when the strain produced by compressing the tuber in both directions was the same, the less stress was required for vertical compression and therefore the vertical direction was more likely to break than the horizontal.

3.3.4. Effect of Variety on Compressive Mechanical Properties

From Table 9, it can be observed that variety had a significant effect on the damage force, deformation, and damage energy of the tubers ($p < 0.01$), and no significant effect on the apparent elastic modulus.

As shown in Figure 9, when the level of factors other than variety was fixed, the damage force and damage energy of variety 2 were generally greater than that of variety 1; variety 2 had more deformation in the vertical direction than variety 1 and less deformation in the lateral direction than variety 1. This was caused by the different shapes and sizes of the varieties, the different contents of the internal substances, etc. [18].

In addition, from Table 9, it can be observed that there were also interactions between the factors that had a significant effect on the different indices of the mechanical properties of compression. In conclusion, in order to reduce the rate of tuber breakage, the effect of factors such as variety, moisture content, and component speed on indicators such as tuber damage force should be taken into account during the design of tuber harvesting and processing machinery.

4. Conclusions

In this study, the frictional, collisional, and compression mechanical properties of tiger nut tubers were researched, and the effects of different factors such as moisture

content on sliding friction coefficient, angle of repose, collision recovery coefficient, damage force, deformation, damage energy, and apparent elastic modulus were analysed, with the following main conclusions:

(1) The effects of moisture content and friction material on the sliding friction coefficient (0.405–0.652) of the tubers were highly significant ($p < 0.01$), with no significant effect of variety. The sliding friction coefficient increased with increasing moisture content when the moisture content was between 8% and 40%. The coefficient of friction between the tuber and the polyurethane, plexiglass, aluminium, and steel plates decreased in descending order when the moisture content was the same. The effect of variety and moisture content on the angle of repose (27.96–36.09°) of tubers was significant ($p < 0.01$); variety 2 had a larger angle of repose than variety 1; and the angle of repose of tubers was positively correlated with moisture content.

(2) The results of the mixed orthogonal test showed that collision material, moisture content, release height, and variety had significant effects($p < 0.01$) on the collision recovery coefficients (0.376–0.672) of the tubers. The results of the single-factor test showed that: when the moisture content increased from 8% to 40%, the recovery coefficient first decreased and then increased, and when the moisture content was 16%, the recovery coefficient was the lowest; when the release height increased from 150 mm to 350 mm, the recovery coefficient gradually decreased; when the levels of other factors were the same, the recovery coefficient of the collision between the tuber and the steel, aluminium, plexiglass, and polyurethane decreased in turn; and influenced by the mass and shape, the recovery coefficient of variety 2 was lower than that of variety 1.

(3) Variety, loading speed, moisture content, and compression direction all had a significant effect on the damage force (87.54–214.48 N), deformation (1.25–6.12 mm), and damage energy (82.38–351.08 mJ) of the tubers ($p < 0.01$), and only moisture content and compression direction had a significant effect on the apparent elastic modulus (12.17~120.88 MPa) of the tubers ($p < 0.01$). When the level of factors other than the loading speed was fixed, the damage force, deformation, and damage energy all tended to decrease as the loading speed increased (from 5 mm/min to 20 mm/min). When the level of factors other than moisture content was fixed, as the moisture content increased (from 16% to 40%), the damage force and apparent elastic modulus increased, the deformation decreased, and the damage energy generally decreased and then increased. When the levels of factors other than the compression direction were fixed, the damage force and apparent elastic modulus were lower in the vertical direction than in the horizontal direction, while the deformation and damage energy were generally higher than in the horizontal direction. When the levels of factors other than variety were fixed, the damage force and damage energy of variety 2 were generally higher than those of variety 1; variety 2 had a higher deformation in the vertical direction than variety 1 and a lower deformation in the horizontal direction than variety 1.

Author Contributions: Conceptualization, S.Z.; methodology, J.F.; validation, R.Z.; investigation, Y.Z.; resources, H.Y.; data curation, S.Z.; writing—original draft preparation, S.Z. All authors have read and agreed to the published version of the manuscript.

Funding: The research was financially supported by the Science and Technology Development Program of Jilin Province, grant, number 20200502007NC, and the Science and Technology Development Program of Jilin Province, grant, number 20200403153SF.

Conflicts of Interest: The authors declare that there is no conflict of interest.

Appendix A

Table A1. Test scheme and results for compression mechanical properties.

V	LS/(mm·min^{-1})	MC/%	Damage Force/N		Deformation/mm		Damage Energy/mJ		Apparent Elastic Modulus/MPa	
			Vertical	Horizontal	Vertical	Horizontal	Vertical	Horizontal	Vertical	Horizontal
V.1	5	16	113.44	153.91	4.54	3.34	155.18	161.30	23.21	45.25
		24	129.37	161.19	4.07	2.54	153.98	125.17	30.68	71.35
		32	137.36	164.65	3.58	2.51	172.53	145.70	39.35	74.57
		40	152.98	177.47	2.64	2.25	181.32	149.65	68.12	93.47
	10	16	106.86	138.46	4.45	2.76	138.80	121.68	22.48	54.07
		24	123.62	142.27	3.84	2.42	139.44	102.66	31.96	67.75
		32	127.89	148.80	3.25	2.37	158.94	126.63	42.24	73.52
		40	147.45	158.20	2.37	2.18	167.42	140.59	77.10	87.49
	15	16	95.12	125.45	4.13	2.62	125.45	102.35	22.43	53.10
		24	109.53	130.09	3.74	2.41	123.41	90.62	29.53	62.58
		32	118.57	135.04	3.48	2.14	147.91	105.88	35.40	77.46
		40	131.85	148.40	2.16	1.68	120.81	98.14	79.63	120.88
	20	16	103.41	118.21	3.74	2.54	121.09	95.22	28.22	52.30
		24	113.48	120.35	3.88	2.34	133.16	82.38	28.93	60.47
		32	109.96	125.84	3.26	2.07	129.85	95.60	36.24	75.82
		40	124.03	136.93	2.07	1.25	118.92	88.28	79.79	107.54
V.2	5	16	124.57	186.00	6.12	2.77	258.77	153.68	14.93	62.69
		24	140.57	194.53	5.09	2.38	257.95	136.98	22.17	83.00
		32	157.25	214.48	4.23	2.22	347.96	169.59	32.58	101.20
		40	172.81	213.28	4.68	1.97	351.08	177.67	34.93	119.37
	10	16	110.03	175.07	5.87	2.59	234.19	133.76	14.05	65.22
		24	135.46	179.55	4.88	2.16	243.56	126.75	22.82	88.46
		32	154.01	187.93	4.19	1.98	304.99	136.89	32.45	104.98
		40	155.08	200.41	3.94	1.93	295.73	156.36	35.79	115.37
	15	16	104.74	163.32	5.81	2.68	230.10	129.60	13.60	57.75
		24	118.55	172.90	4.99	2.19	219.09	107.95	19.29	83.44
		32	144.60	177.75	3.90	1.96	277.16	129.68	33.92	100.81
		40	146.39	182.92	3.81	1.78	253.35	139.88	35.51	119.32
	20	16	87.54	160.56	5.56	2.55	213.04	127.95	12.17	61.20
		24	101.49	168.57	4.82	2.01	188.53	104.53	17.41	92.53
		32	115.60	169.60	4.13	1.92	214.63	105.85	24.86	99.21
		40	140.09	173.32	3.76	1.75	222.64	120.91	34.67	115.09

Note: V shows variety; LS shows loading speed; MC shows moisture content; and CD shows the the compression direction.

References

1. Wang, R.Y.; Wang, X.S.; Xiang, H. A multi-purpose novel oil crop—Cyperus Edulis. *China Oils Fats* **2019**, *44*, 1–4. (In Chinese with English Abstract)
2. Zhao, X.Q.; Liu, H.; Lu, Z.Y.; Cheng, Y.C.; Zhang, D.J.; Bai, L.F.; Fang, J.; Du, X.Y.; Ren, Y.F. Cultivation techniques for sand control and sand fixation on sandy degraded land with Cyperus beans. *Mod. Agric.* **2019**, *516*, 14–15. (In Chinese with English Abstract) [CrossRef]
3. Yang, F.; Zhu, W.X. Research status and prospect of *Cyperus esculentus*. *Cereals Oils* **2020**, *33*, 4–6. (In Chinese with English Abstract)
4. Liu, Y.L.; Wang, X.N.; Shu, Y.; Ma, Y.X. Character and composition of *Cyperus esculentus* from different origins. *China Oils Fats* **2020**, *45*, 125–129. (In Chinese with English Abstract) [CrossRef]
5. Zhang, B.; Liu, J.; Fang, Z.X.; Hou, P.L.; Fu, J.; Guo, F.D.; Hou, L.; Ma, D.Y.; Wang, Y. Research progresses of mechanical seeding and harvesting technology and equipment for Saline-Alkali *Cyperus esculentus*. *Shandong Agric. Sci.* **2019**, *51*, 144–148. (In Chinese with English Abstract) [CrossRef]
6. Abano, E.E.; Amoah, K.K. Effect of Moisture Content on the Physical Properties of Tiger Nut (*Cyperus esculentus*). *Asian J. Agric. Res.* **2011**, *5*, 56–66. [CrossRef]
7. Wang, L.; Hu, C.; Guo, W.S.; He, X.W.; Wang, X.F.; Jian, J.M.; Hou, S.L. The Effects of Moisture Content and Loading Orientation on Some Physical and Mechanical Properties of Tiger Nut. *Am. J. Biochem. Biotechnol.* **2021**, *17*, 109–117. [CrossRef]
8. Chen, Z.P.; Wassgren, C.; Veikle, E.; Ambrose, K. Determination of material and interaction properties of maize and wheat kernels for DEM simulation. *Biosyst. Eng.* **2020**, *195*, 208–226. [CrossRef]

9. Chandio, F.A.; Li, Y.M.; Ma, Z.; Ahmad, F.; Syed, T.N.; Shaikh, S.A.; Tunio, M.H. Influences of moisture content and compressive loading speed on the mechanical properties of maize grain orientations. *Int. J. Agric. Biol. Eng.* **2021**, *14*, 41–49. [CrossRef]
10. Feng, B.; Sun, W.; Shi, L.R.; Sun, B.G.; Zhang, T.; Wu, J.M. Determination of restitution coefficient of potato tubers collision in harvest and analysis of its influence factors. *Trans. CSAE* **2017**, *33*, 50–57. (In Chinese with English Abstract) [CrossRef]
11. Liu, W.Z.; He, J.; Li, H.W.; Li, X.Q.; Zheng, K.; Wei, Z.C. Calibration of simulation parameters for potato minituber based on EDEM. *Trans. CSAM* **2018**, *49*, 125–135. (In Chinese with English Abstract) [CrossRef]
12. Meng, J.G.; Wang, C.G.; Xie, S.S.; Deng, W.G.; Qi, S.H.; Li, J. Test and analysis of restitution coefficient of potato. *J. China Agric. Univ.* **2017**, *22*, 93–100. (In Chinese with English Abstract) [CrossRef]
13. Sun, J.X.; Yang, Z.M.; Guo, Y.M.; Cui, Q.L.; Wu, X.H.; Zhang, Y.Q. Compression mechanical properties and crack formation law of millet grain. *Trans. CSAE* **2017**, *33*, 306–314. (In Chinese with English Abstract) [CrossRef]
14. Gao, L.X.; Jiao, W.P.; Yang, D.X.; Shao, Z.G.; Zhao, X.G.; Liu, D.J. Effect of oisture content on mechanical properties of soybean seed under static pressure. *Trans. CSAE* **2012**, *28*, 40–44. (In Chinese with English Abstract) [CrossRef]
15. Arslan, S.; Vursavus, K.K. Physico-Mechanical Properties of Almond Nut and Its Kernel as a Function of Variety and Moisture Content. *Philipp. Agric.* **2009**, *91*, 171–179. [CrossRef]
16. Zhang, H.; Shen, L.Y.; Lan, H.P.; Li, Y.; Liu, Y.; Tang, Y.R.; Li, W. Mechanical properties and finite element analysis of walnut under different cracking parts. *Int. J. Agric. Biol. Eng.* **2018**, *11*, 81–88. [CrossRef]
17. He, J.C.; Tao, Z.Y.; Liang, S.H.; Ye, D.P. Compression and shearing force on kernel rupture in shelling fresh lotus seeds. *Int. J. Agric. Biol. Eng.* **2021**, *14*, 237–242. [CrossRef]
18. Kamst, G.F.; Bonazzi, C.; Vasseur, J.; Bimbenet, J.J. Effect of deformation rate and moisture content on the mechanical properties of rice grains. *Trans. ASAE* **2002**, *45*, 145–151. [CrossRef]
19. Na, X.J.; Liu, M.G.; Zhang, W.; Li, F.; Du, X.; Gao, L.X. Damage characteristics and regularity of peanut kernels under mechanical shelling. *Trans. CSAE* **2010**, *5*, 117–121. (In Chinese with English Abstract) [CrossRef]
20. Jing, S.Q.; Wang, S.S.; Li, Q.; Zheng, L.; Yue, L.; Fan, S.L.; Tao, G.Y. Dynamic high pressure microfluidization-assisted extraction and bioactivities of *Cyperus esculentus* (*C. esculentus* L.) leaves flavonoids. *Food Chem.* **2016**, *192*, 319–327. [CrossRef]
21. Hu, B.; Zhou, K.; Liu, Y.T.; Liu, A.P.; Zhang, Q.; Han, G.Q. Optimization of microwave-assisted extraction of oil from tiger nut (*Cyperus esculentus* L.) and its quality evaluation. *Ind. Crops Prod.* **2018**, *115*, 290–297. [CrossRef]
22. Liu, H.M.; Yan, Y.Y.; Liu, X.X.; Ma, Y.X.; Wang, X.D. Effects of various oil extraction methods on the gelatinization and retrogradation properties of starches isolated from tigernut (*Cyperus esculentus*) tuber meals. *Int. J. Biol. Macromol.* **2020**, *156*, 144–152. [CrossRef]
23. Asante, F.A.; Ellis, W.O.; Oduro, I.; Saalia, F.K. Effect of Soaking and Cooking Methods on Extraction of Solids and Acceptability of Tiger Nut (*Cyperus Esculentus* L.) Milk. *J. Agric. Stud.* **2014**, *2*, 76–86. [CrossRef]
24. Gasparre, N.; Pan, J.; Alves, P.L.D.S.; Rosell, C.M.; Berrios, J.D.J. Tiger Nut (*Cyperus esculentus*) as a Functional Ingredient in Gluten-Free Extruded Snacks. *Foods* **2020**, *9*, 1770. [CrossRef] [PubMed]
25. Aguilar, N.; Albanell, E.; Miñarro, B.; Guamis, B.; Capellas, M. Effect of tiger nut-derived products in gluten-free batter and bread. *Food Sci. Technol. Int.* **2015**, *21*, 323–331. [CrossRef] [PubMed]
26. Ahmed, Z.S.; Hussein, A.M.S. Exploring the Suitability of Incorporating Tiger Nut Flour as Novel Ingredient in Gluten-Free Biscuit. *Pol. J. Food Nutr. Sci.* **2014**, *64*, 27–33. [CrossRef]
27. Kizzie-Hayford, N.; Dabie, K.; Kyei-Asante, B.; Ampofo-Asiama, J.; Zahn, S.; Jaros, D.; Rohm, H. Storage temperature of tiger nuts (*Cyperus esculentus* L.) affects enzyme activity, proximate composition and properties of lactic acid fermented tiger nut milk thereof. *LWT* **2021**, *137*. [CrossRef]
28. Yao, N.J.C.; Augustin, A.A.; Niamke, B.F.; Adje, A.F. Composition of Fatty Acids, Total Sterols and Total Polyphenol Content of the Oils of Six Oilseeds in Côte d'Ivoire. *Asian Food Sci. J.* **2020**, *19*, 1–9. [CrossRef]
29. Ezeh, O.; Gordon, M.H.; Niranjan, K. Enhancing the recovery of tiger nut (*Cyperus esculentus*) oil by mechanical pressing: Moisture content, particle size, high pressure and enzymatic pre-treatment effects. *Food Chem.* **2016**, *194*, 354–361. [CrossRef]
30. Okorie, S.U.; Adedokun, I.I.; Duru, N.H. Effect of Blending and Storage Conditions on the Microbial Quality and Sensory Characteristics of Soy-Tiger Nut Milk Beverage. *Food Sci. Qual. Manag.* **2014**, *31*, 96–103.
31. Bezuidenhout, S.R.; Reinhardt, C.F.; Whitwell, M.I. Cover crops of oats, stooling rye and three annual ryegrass cultivars influence maize and *Cyperus esculentus* growth. *Weed Res.* **2012**, *52*, 153–160. [CrossRef]
32. Cui, Q.; Wang, L.; Wang, G.R.; Zhang, A.Q.; Wang, X.B.; Jiang, L.Z. Ultrasonication effects on physicochemical and emulsifying properties of *Cyperus esculentus* seed (tiger nut) proteins. *LWT* **2021**, *142*. [CrossRef]
33. Shrestha, U.; Rosskopf, E.N.; Butler, D.M. Effect of anaerobic soil disinfestation amendment type and C:N ratio on *Cyperus esculentus* tuber sprouting, growth and reproduction. *Weed Res.* **2018**, *58*, 379–388. [CrossRef]
34. Chloe, J. P29 The in vitro use of natural antioxidant oils (*Cyperus esculentus*; *Nigella sativa*) to reduce cell sickling in sickle cell anaemia. *Biochem. Pharmacol.* **2017**, *139*, 134. [CrossRef]
35. Jia, H.L.; Deng, J.Y.; Deng, Y.L.; Chen, T.Y.; Wang, G.; Sun, Z.J.; Guo, H. Contact parameter analysis and calibration in discrete element simulation of rice straw. *Int. J. Agric. Biol. Eng.* **2021**, *14*, 72–81. [CrossRef]
36. Shi, L.R.; Ma, Z.T.; Zhao, W.Y.; Yang, X.P.; Sun, B.G.; Zhang, J.P. Calibration of simulation parameters of flaxed seeds using discrete element method and verification of seed-metering test. *Trans. CSAE* **2019**, *35*, 25–33. (In Chinese with English Abstract) [CrossRef]